Polyhedron 30 (2011) 2896–2907

Contents lists available at SciVerse ScienceDirect

Polyhedron

journal homepage: www.elsevier.com/locate/poly

Phosphorus–nitrogen compounds part 22. Syntheses, structural investigations, biological activities and DNA interactions of new mono and bis (4-fluorobenzyl) spirocyclophosphazenes

Aytuğ Okumuş [a], Zeynel Kılıç [a,*], Tuncer Hökelek [b], Hakan Dal [c], Leyla Açık [d], Yağmur Öner [d], L. Yasemin Koç [e]

[a] Department of Chemistry, Ankara University, 06100 Tandoğan-Ankara, Turkey
[b] Department of Physics, Hacettepe University, 06800 Beytepe-Ankara, Turkey
[c] Department of Chemistry, Anadolu University, 26470 Yunus Emre Kampüsü-Eskişehir, Turkey
[d] Department of Biology, Gazi University, 06500 Teknikokullar-Ankara, Turkey
[e] Department of Biology, Ankara University, 06100 Tandoğan-Ankara, Turkey

ARTICLE INFO

Article history:
Received 30 April 2011
Accepted 24 August 2011
Available online 8 September 2011

Keywords:
Fluorobenzylspirocyclophosphazenes
Spectroscopy
Crystal structure
Antimicrobial activity
DNA cleavage

ABSTRACT

The reactions of hexachlorocyclotriphosphazene, $N_3P_3Cl_6$, with mono (**1** and **2**) and bis(4-fluorobenzyl) diamines (**3**-**5**), $FPhCH_2NH(CH_2)_nNHR$ (R=H or $FPhCH_2$–), produce mono (**1a** and **2a**) and bis(4-fluorobenzyl) monospirocyclophosphazenes (**3a**–**5a**). The tetraaminomonospirocyclophosphazenes (**1b**–**2d**) are obtained from the reactions of the partly substituted phosphazenes (**1a** and **2a**) with excess pyrrolidine, morpholine and 1,4-dioxa-8-azaspiro[4,5]decane (DASD), respectively. The tetrachlorobis(4-fluorobenzyl) monospirocyclophosphazenes (**4a** and **5a**) with excess pyrrolidine, morpholine and DASD afford the fully substituted bis(4-fluorobenzyl) monospirocyclophosphazenes (**4b**, **4d**–**5d**) in boiling THF. In addition, monochlorobis(4-fluorobenzyl) monospirocyclophosphazenes (**4e** and **4f**) have also been isolated from the reactions with excess morpholine and DASD in boiling THF. The structural investigations of the compounds have been verified by elemental analyses, MS, FTIR, ^1H, ^{13}C, ^{19}F (for **1d** and **2d**), ^{31}P NMR, HSQC and HMBC techniques. The crystal structures of **3a**, **4a**, **5a** and **2b** have been determined by X-ray crystallography. The compounds **2a**–**5a**, **1b**–**2d**, **4b**, **4d**–**5d**, **4e** and **4f** have been screened for antibacterial effects on bacteria and for antifungal activity against yeast strains. The compounds **1b** and **4b** showed antimicrobial activity against three species of bacteria, *Bacillus subtilis, Bacillus cereus* and *Staphylococcus aureus*, and two fungi, *Candida albicans* and *Candida tropicalis*. Minimum inhibitory concentrations (MIC) were determined for **1b** and **4b**. The MIC values were found to be 5000 μM for each bacteria. The most effective compound, **4b** has exhibited activity with a MIC of 312 μM for *C. albicans* and 625 μM for *C. tropicalis*. DNA-binding and the nature of the interaction with pBR322 plasmid DNA are studied. All of the compounds induce changes on the DNA mobility and intensity. Prevention of *Hind*III digestion with the compounds indicates that the compounds bind with AT nucleotides in DNA.

1. Introduction

The word phosphazene refers to a broad range of molecules, containing phosphorus and nitrogen atoms attached by regularly PN bonds. The PN units are joined together to form either short and long chains or cyclophosphazenes. The hexachlorocyclotriphosphazene, $N_3P_3Cl_6$, is the best known starting compound and the most extensively studied in the field of phosphazene chemistry. In the last decade, there has been a considerable amount of interest in the syntheses of spirocyclic phosphazenes in general and in the determination of the stereogenic properties of chiral cyclophosphazenes in particular [1,2]. Most of the phosphazene derivatives have been prepared by chloride replacement reactions on $N_3P_3Cl_6$, due to the ease of introducing a wide variety of organic, inorganic and organometallic groups onto the P centers [3–5]. On the other hand, cyclophosphazenes are intensively used as building blocks for polyorganophosphazenes, such as open-chain, cyclolinear, cyclomatrix polymers and dendrimers [6–8]. The properties of linear polyorganophosphazenes especially depend on the inorganic PN skeleton as well as on the nature of the substituents attached to the phosphorus atoms [9,10]. Moreover, they have been prepared for use in alternative industrial applications in different areas, for instance in rechargeable lithium batteries and polymer electrolytes [11,12], high performance elastomers [13], non-linear optics [14,15], biomedical membranes [16] and

* Corresponding author. Tel.: +90 3122126720 1043; fax: +90 3122232395.
E-mail address: zkilic@science.ankara.edu.tr (Z. Kılıç).

0277-5387/$ - see front matter © 2011 Elsevier Ltd. All rights reserved.
doi:10.1016/j.poly.2011.08.035

biomedical materials including synthetic bones [17]. Recently, our group has focused on the replacement reactions of the Cl atoms of $N_3P_3Cl_6$ by bulky aromatic diamines [18], N_xO_y-donor type (x, y = 2–4) dibenzo-diaza-crown ethers (coronands) [19], diaminophenolates [20–22] and ferrocenyldiamines [23] to obtain novel phosphazene derivatives with different architectures, namely *spiro*-, *ansa*-, di*spiro*-, tri*spiro*-, *spiro-ansa*-, *spiro-ansa-spiro*-, *spiro-bino-spiro*- and *spiro*-crypta-skeletons. As far as we are aware, there is no report on the reactions of difunctional reagents containing pendant 4-fluorobenzyl groups. Thus, this study primarily focuses on the substitution reactions of $N_3P_3Cl_6$ with mono and bis(4-fluorobenzyl) diamines with the aim of the preparation of possible biologically active phosphazene derivatives.

We report here (i) the syntheses of new mono (**1a**, **2a**, **1b**–**2d**) and bis(4-fluorobenzyl) monospirocyclo phosphazenes (**3a**–**5a**, **4b**, **4d**–**4f**, **5b**–**5d**) (Scheme 1), (ii) the determination of the structures of all the compounds by elemental analyses, mass spectrometry, Fourier transform (FTIR), one-dimensional (1D) ^{1}H, ^{13}C, ^{19}F (for **1d** and **2d**) and ^{31}P NMR, two-dimensional (2D) heteronuclear single quantum coherence (HSQC), and heteronuclear multiple-bond correlation (HMBC) techniques; (iii) the solid-state structures of **3a**, **4a**, **5a** and **2b**, established by X-ray diffraction techniques; (iv) investigations of antibacterial and antifungal activities of **2a**–**5a**, **1b**–**2d**, **4b**, **4d**–**5d**, **4e** and **4f** and (v) the interactions between these compounds and pBR322 plasmid DNA examined by agarose gel electrophoresis.

2. Experimental

2.1. General methods

The reactions have been monitored using thin-layer chromatography (TLC) in different solvents, and the experiments were carried out under an argon atmosphere. The melting points were measured on a Gallenkamp apparatus using a capillary tube. The IR spectra were recorded on a Jasco FT/IR-430 spectrometer in KBr discs and are reported in cm^{-1} units. Mass spectra are recorded on an AGILEND 1100 MSD spectrometer using the API-ES method. Elemental analyses were carried out by the microanalytical service of TÜBİTAK-Turkey. ^{1}H, ^{13}C, ^{19}F, ^{31}P, HSQC and HMBC spectra were recorded on a Bruker DPX FT NMR (400 MHz) spectrometer ($SiMe_4$ as an internal standard for ^{1}H, $CFCl_3$ as an internal standard for ^{19}F and 85% H_3PO_4 as an external standard for ^{31}P NMR), operating at 400.13, 100.62, 376.46, and 161.97 MHz. The spectrometer was equipped with a 5 mm PABBO BB inverse-gradient probe. Standard

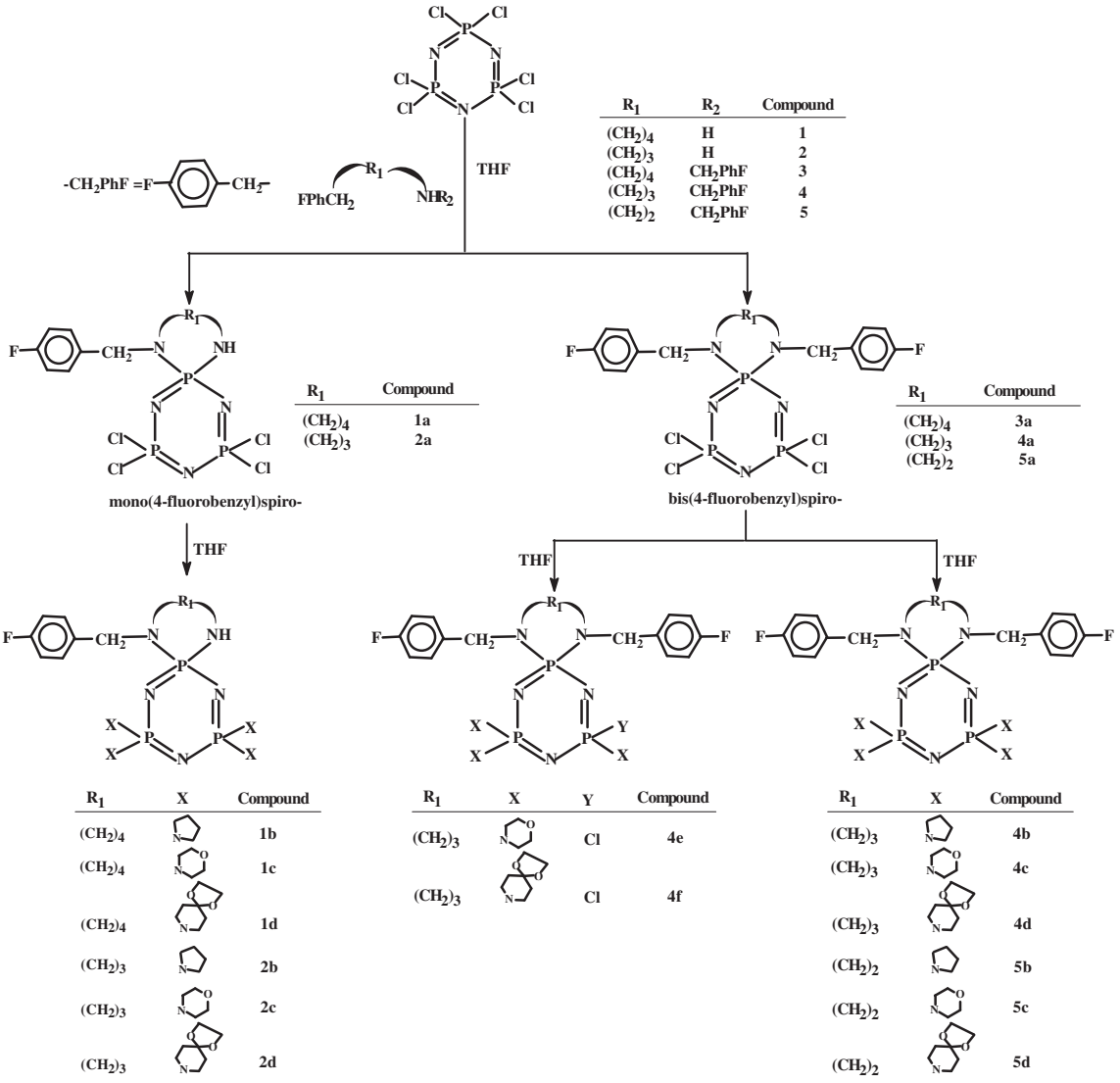

Scheme 1. The chloride replacement reaction pathway of $N_3P_3Cl_6$ with mono and bis(4-fluorobenzyl) diamines, pyrrolidine, morpholine and DASD.

Bruker pulse programs [24] were used. Antimicrobial susceptibility testing was performed by the disk diffusion method. The DNA binding abilities were examined using agarose gel electrophoresis [2,23].

2.2. Preparation of Compounds

The 4-fluorobenzyldiamines (**1**–**5**) were obtained by the reduction of the corresponding Schiff bases prepared from the reaction of 4-fluorobenzyaldehyde with the appropriate diamines in methanol according to the methods reported in the literature [25,26].

2.2.1. 2,2,4,4-Tetrachloro-7-(4-fluorobenzyl)-1,3,5,7,12-pentaaza-2λ⁵,4λ⁵,6λ⁵-triphosphaspiro[5.6]trideca-1,3,5-triene (*1a*)

A solution of **1** (1.00 g, 5.10 mmol) in THF (150 mL) and triethylamine (1.42 mL) was added to a stirred solution of $N_3P_3Cl_6$ (1.78 g, 5.10 mmol) in THF (50 mL) at room temperature. The mixture was stirred for 25 h at ambient temperature, with argon being passed over the reaction mixture. The precipitated amine hydrochloride was filtered off, and the solvent was evaporated at reduced pressure. The crude product was purified by column chromatography with toluene. A white powder crystallized out from toluene. Yield: 1.56 g (65%). M.p.: 122 °C. *Anal.* Calc. for $C_{11}H_{15}N_5FP_3Cl_4$: C, 28.05; H, 3.18; N, 14.86. Found: C, 28.77; H, 3.34; N, 14.59%. APIES-MS (fragments are based on ^{35}Cl, Ir%): *m*/z 469 ($[M]^+$, 79.8). FTIR (KBr, cm^{-1}): 3068, 3022 (C–H arom.), 1055 (C–F), 1236, 1186 (P═N), 568, 518 (PCl).

2.2.2. 2,2,4,4-Tetrachloro-7-(4-fluorobenzyl)-1,3,5,7,11-pentaaza-2λ⁵,4λ⁵,6λ⁵-triphosphaspiro[5.5]undeca-1,3,5-triene (*2a*)

The procedure was as for compound **1a**, using **2** (1.00 g, 5.49 mmol), and triethylamine (1.53 mL) and $N_3P_3Cl_6$ (1.91 g, 5.49 mmol) (26 h). The product was purified by column chromatography using toluene and crystallized from toluene. Yield: 1.75 g (70%). M.p.: 68 °C. *Anal.* Calc. for $C_{10}H_{13}N_5FP_3Cl_4$: C, 26.29; H, 2.87; N, 15.33. Found: C, 26.38; H, 2.91; N, 15.23%. APIES-MS (fragments are based on ^{35}Cl, Ir%): *m*/z 455 ($[M]^+$, 0.2). FTIR (KBr, cm^{-1}): 3070, 3048 (C–H arom.), 1051 (C–F), 1228, 1178 (P═N), 570, 510 (PCl).

2.2.3. 2,2,4,4-Tetrachloro-7,12-bis(4-fluorobenzyl)-1,3,5,7,12-pentaaza-2λ⁵,4λ⁵,6λ⁵-triphosphaspiro[5.6]trideca-1,3,5-triene (*3a*)

The procedure was as for compound **1a**, using **3** (0.1 g, 3.29 mmol), and triethylamine (0.55 mL) and $N_3P_3Cl_6$ (0.11 g, 3.29 mmol) (26 h). The product was purified by column chromatography using toluene and crystallized from toluene. Yield: 0.12 g (63%). M.p.: 177 °C. *Anal.* Calc. for $C_{18}H_{20}N_5F_2P_3Cl_4$: C, 37.33; H, 3.48; N, 12.09. Found: C, 37.53; H, 3.61; N, 12.18%. APIES-MS (fragments are based on ^{35}Cl, Ir%): *m*/z 577 ($[M]^+$, 56.5). FTIR (KBr, cm^{-1}): 3072, 3043 (C–H arom.), 1051 (C–F), 1224, 1182 (P═N), 567, 514 (PCl).

2.2.4. 2,2,4,4-Tetrachloro-7,11-bis(4-fluorobenzyl)-1,3,5,7,11-pentaaza-2λ⁵,4λ⁵,6λ⁵-triphosphaspiro[5.5]undeca-1,3,5-triene (*4a*)

The procedure was as for compound **1a**, using **4** (0.50 g, 1.72 mmol), and triethylamine (0.96 mL) and $N_3P_3Cl_6$ (0.60 g, 1.72 mmol) (26 h). The product was purified by column chromatography using toluene and crystallized from toluene. Yield: 0.66 g (68%). M.p.: 108 °C. *Anal.* Calc. for $C_{17}H_{18}N_5FP_3Cl_4$: C, 36.13; H, 3.21; N, 12.39. Found: C, 36.45; H, 3.28; N, 12.33%. APIES-MS (fragments are based on ^{35}Cl, Ir%): *m*/z 563 ($[M]^+$, 49.1). FTIR (KBr, cm^{-1}): 3064, 3030 (C–H arom.), 1052 (C–F), 1228, 1172 (P═N), 579, 517 (PCl).

2.2.5. 7,10-Bis(4-fluorobenzyl)-2,2,4,4-tetrachloro-1,3,5,7,10-pentaaza-2λ⁵,4λ⁵,6λ⁵-triphosphaspiro[4.5]dodeca-1,3,5-triene (*5a*)

The procedure was as for compound **1a**, using **5** (1.02 g, 3.70 mmol), and triethylamine (1.03 mL) and $N_3P_3Cl_6$ (1.29 g, 3.70 mmol) (26 h). The product was purified by column chromatography using toluene and crystallized from toluene. Yield: 2.04 g (74%). M.p.: 146 °C. *Anal.* Calc. for $C_{16}H_{16}N_5F_2P_3Cl_4$: C, 34.87; H, 2.93; N, 12.71. Found: C, 35.19; H, 3.03; N, 12.79%. APIES-MS (fragments are based on ^{35}Cl, Ir%): *m*/z 550 ($[M]^+$, 56.3). FTIR (KBr, cm^{-1}): 3072, 3020 (C–H arom.), 1059 (C–F), 1227, 1190 (P═N), 574, 512 (PCl).

2.2.6. 7-(4-Fluorobenzyl)-2,2,4,4-tetrapyrrolidin-1-yl-1,3,5,7,12-pentaaza-2λ⁵,4λ⁵,6λ⁵-triphosphaspiro[5.6]trideca-1,3,5-triene (*1b*)

A solution of compound **1a** (1.00 g, 2.12 mmol) and triethylamine (1.18 mL) in dry THF (150 mL) was added slowly to a solution of pyrrolidine (2.10 mL, 26.00 mmol) with stirring, and then the mixture was refluxed for 34 h. The oily product was purified by column chromatography using toluene-THF (1:4) as eluent and then crystallized from *n*-heptane. Yield: 0.94 g (73%). M.p.: 107 °C. *Anal.* Calc. for $C_{27}H_{47}N_9FP_3$: C, 53.20; H, 7.77; N, 20.68. Found: C, 51.61; H, 7.41; N, 20.00%. APIES-MS (fragments are based on ^{35}Cl, Ir%): *m*/z 610 ($[M]^+$, 100). FTIR (KBr, cm^{-1}): 3068, 3022 (C–H arom.), 1056 (C–F), 1236, 1198 (P═N).

2.2.7. 7-(4-Fluorobenzyl)-2,2,4,4-tetramorpholin-4-yl-1,3,5,7,12-pentaaza-2λ⁵,4λ⁵,6λ⁵-triphosphaspiro[5.6]trideca-1,3,5-triene (*1c*)

The procedure was similar to that of compound **1b**, using **1a** (0.98 g, 2.07 mmol), morpholine (2.17 mL, 25.00 mmol) and triethylamine (1.16 mL) (35 h). The product was purified by column chromatography using toluene-THF (1:4) and crystallized from *n*-heptane. Yield: 0.98 g (70%). M.p.: 157 °C. *Anal.* Calc. for $C_{27}H_{47}N_9FP_3O_4$: C, 53.33; H, 7.18; N, 16.46. Found: C, 51.93; H, 7.12; N, 16.31%. APIES-MS (fragments are based on ^{35}Cl, Ir%): *m*/z 674 ($[M]^+$, 100). FTIR (KBr, cm^{-1}): 3053, 3030 (C–H arom.), 1054 (C–F), 1230, 1194 (P═N).

2.2.8. 7-(4-Fluorobenzyl)-2,2,4,4-tetra-1,4-dioxa-8-azaspiro[4.5]dec-8-yl-1,3,5,7,12-pentaaza-2λ⁵,4λ⁵,6λ⁵-triphosphaspiro[5.6]trideca-1,3,5-triene (*1d*)

The procedure was similar to that of compound **1b**, using **1a** (1.00 g, 2.12 mmol), DASD (3.26 mL, 26.00 mmol) and triethylamine (1.18 mL) (35 h). The product was purified by column chromatography using toluene-THF (1:4) and crystallized from *n*-heptane. Yield: 1.38 g (72%). M.p.: 174 °C. *Anal.* Calc. for $C_{39}H_{63}N_9FP_3O_8$: C, 52.20; H, 7.07; N, 14.03. Found: C, 52.75; H, 6.67; N, 13.01%. APIES-MS (fragments are based on ^{35}Cl, Ir%): *m*/z 898 ($[M]^+$, 91.9). FTIR (KBr, cm^{-1}): 3064, 3033 (C–H arom.), 1052 (C–F), 1210, 1188 (P═N).

2.2.9. 7-(4-Fluorobenzyl)-2,2,4,4-tetrapyrrolidin-1-yl-1,3,5,7,11-pentaaza-2λ⁵,4λ⁵,6λ⁵-triphosphaspiro[5.5]undeca-1,3,5-triene (*2b*)

The procedure was similar to that of compound **1b**, using **2a** (0.70 g, 1.53 mmol), pyrrolidine (1.52 mL, 18.00 mmol) and triethylamine (0.85 mL) (36 h). The product was purified by column chromatography using toluene-THF (1:4) and crystallized from toluene. Yield: 0.69 g (76%). M.p.: 106 °C. *Anal.* Calc. for $C_{26}H_{45}N_9FP_3$: C, 52.43; H, 7.62; N, 21.16. Found: C, 52.25; H, 7.48; N, 21.03%. APIES-MS (fragments are based on ^{35}Cl, Ir%): *m*/z 596 ($[M]^+$, 100). FTIR (KBr, cm^{-1}): 3062, 3021 (C–H arom.), 1051 (C–F), 1230, 1182 (P═N).

2.2.10. 7-(4-Fluorobenzyl)-2,2,4,4 tetramorpholin-4-yl-1,3,5,7,11-pentaaza-2λ⁵,4λ⁵,6λ⁵-triphosphaspiro[5.5]undeca-1,3,5-triene (*2c*)

The procedure was similar to that of compound **1b**, using **2a** (0.70 g, 1.53 mmol), morpholine (1.60 mL, 18.00 mmol) and

triethylamine (0.85 mL) (37 h). The product was purified by column chromatography using toluene-THF (1:4) and crystallized from *n*-heptane. Yield: 0.65 g (65%). M.p.: 183 °C. *Anal.* Calc. for $C_{26}H_{45}N_9FP_3O_4$: C, 47.34; H, 6.86; N, 19.11. Found: C, 49.07; H, 6.73; N, 17.03%. APIES-MS (fragments are based on ^{35}Cl, Ir%): *m*/z 660 ($[M]^+$, 100). FTIR (KBr, cm^{-1}): 3059, 3035 (C–H arom.), 1050 (C–F), 1230, 1190 (P=N).

*2.2.11. 7-(4-Fluorobenzyl)-2,2,4,4-tetra-1,4-dioxa-8-azaspiro[4.5]dec-8-yl-1,3,5,7,11-pentaaza-2λ^5,4λ^5,6λ^5-triphosphaspiro[5.5]undeca-1,3,5-triene (**2d**)*

The procedure was similar to that of compound **1b**, using **2a** (0.60 g, 1.30 mmol), DASD (2.00 mL, 16.00 mmol) and triethylamine (0.73 mL) (37 h). The product was purified by column chromatography using toluene-THF (1:4) and crystallized from *n*-heptane. Yield: 0.85 g (73%). M.p.: 223 °C. *Anal.* Calc. for $C_{38}H_{61}N_9FP_3O_8$: C, 51.60; H, 6.96; N, 14.26. Found: C, 52.03; H, 6.87; N, 13.83%. APIES-MS (fragments are based on ^{35}Cl, Ir%): *m*/z 884 ($[M]^+$, 100). FTIR (KBr, cm^{-1}): 3064, 3037 (C–H arom.), 1052 (C–F), 1220, 1192 (P=N).

*2.2.12. 7,11-Bis(4-fluorobenzyl)-2,2,4,4-tetrapyrrolidin-1-yl-1,3,5,7,11-pentaaza-2λ^5,4λ^5,6λ^5-triphosphaspiro[5.5]undeca-1,3,5-triene (**4b**)*

The procedure was similar to that of compound **1b**, using **4a** (1.08 g, 1.91 mmol), pyrrolidine (1.89 mL, 23.00 mmol) and triethylamine (1.06 mL) (30 h). The product was purified by column chromatography using toluene-THF (1:1) and crystallized from *n*-heptane. Yield: 0.99 g (74%). M.p.: 87 °C. *Anal.* Calc. for $C_{33}H_{50}N_9F_2P_3$: C, 56.35; H, 7.16; N, 17.92. Found: C, 56.13; H, 7.03; N, 17.72%. APIES-MS (fragments are based on ^{35}Cl, Ir%): *m*/z 704 ($[M]^+$, 100). FTIR (KBr, cm^{-1}): 3062, 3034 (C–H arom.), 1054 (C–F), 1218, 1182 (P=N).

*2.2.13. 7,11-Bis(4-fluorobenzyl)-2,2,4,4-tetra-1,4-dioxa-8-azaspiro[4.5]dec-8-yl-1,3,5,7,11-pentaaza-2λ^5,4λ^5,6λ^5-triphosphaspiro[5.5]undeca-1,3,5-triene (**4d**)*

A solution of compound **4a** (1.06 g, 1.90 mmol) and triethylamine (1.00 mL) in dry o-xylene (150 mL) was added slowly to a solution of DASD (1.86 mL, 21.00 mmol) with stirring, and then the mixture was refluxed for 32 h. The oily product was purified by column chromatography using toluene-THF (1:1) as the eluent and then was crystallized from *n*-heptane. Yield: 1.34 g (72%). M.p.: 222 °C. *Anal.* Calc. for $C_{45}H_{66}N_9F_2P_3O_8$: C, 54.49; H, 6.71; N, 12.71. Found: C, 53.81; H, 6.44; N, 12.67%. APIES-MS (fragments are based on ^{35}Cl, Ir%): *m*/z 992 ($[M]^+$, 100). FTIR (KBr, cm^{-1}): 3068, 3041 (C–H arom.), 1052 (C–F), 1219, 1195 (P=N).

*2.2.14. 7,11-Bis(4-fluorobenzyl)-2-chloro-2,4,4-trimorpholin-4-yl-1,3,5,7,11-pentaaza-2λ^5,4λ^5,6λ^5-triphosphaspiro[5.5]undeca-1,3,5-triene (**4e**)*

The procedure was similar to that of compound **1b**, using **4a** (1.00 g, 1.78 mmol), morpholine (1.86 mL, 21.00 mmol) and triethylamine (1.00 mL) (32 h). The product was purified by column chromatography using toluene-THF (1:1) and crystallized from *n*-heptane. Yield: 0.88 g (69%). M.p.: 108 °C. *Anal.* Calc. for $C_{29}H_{42}N_8F_2P_3O_3Cl$: C, 48.57; H, 5.90; N, 15.62. Found: C, 48.43; H, 6.14; N, 13.56%. APIES-MS (fragments are based on ^{35}Cl, Ir%): *m*/z 716 ($[M]^+$, 0.8). FTIR (KBr, cm^{-1}): 3056, 3034 (C–H arom.), 1056 (C–F), 1228, 1194 (P=N), 500 (PCl).

*2.2.15. 7,11-Bis(4-fluorobenzyl)-2-chloro-2,4,4-tri-1,4-dioxa-8-azaspiro[4.5]dec-8-yl-1,3,5,7,11-pentaaza-2λ^5,4λ^5,6λ^5-triphosphaspiro[5.5]undeca-1,3,5-triene (**4f**)*

The procedure was similar to that of compound **1b**, using **4a** (1.00 g, 1.78 mmol), DASD (1.86 mL, 21.00 mmol) and triethylamine (1.00 mL) (33 h). The product was purified by column chromatography using toluene-THF (1:1) and crystallized from *n*-heptane. Yield: 0.88 g (69%). M.p.: 166 °C. *Anal.* Calc. for $C_{38}H_{54}N_8F_2P_3O_6Cl$: C, 51.56; H, 6.15; N, 12.66. Found: C, 52.78; H, 6.27; N, 12.16%. APIES-MS (fragments are based on ^{35}Cl, Ir%): *m*/z 884 ($[M]^+$, 2.0). FTIR (KBr, cm^{-1}): 3075, 3041 (C–H arom.), 1056 (C–F), 1219, 1194 (P=N), 577 (PCl).

*2.2.16. 7,10-Bis(4-fluorobenzyl)-2,2,4,4-tetrapyrrolidin-1-yl-1,3,5,7,10-pentaaza-2λ^5,4λ^5,6λ^5-triphosphaspiro[4.5]dodeca-1,3,5-triene (**5b**)*

The procedure was similar to that of compound **1b**, using **5a** (1.07 g, 1.94 mmol), pyrrolidine (1.93 mL, 23.00 mmol) and triethylamine (1.09 mL) (30 h). The product was purified by column chromatography using toluene-THF (1:1) and crystallized from *n*-heptane. Yield: 1.09 g (81%). M.p.: 207 °C. *Anal.* Calc. for $C_{32}H_{48}N_9F_2P_3$: C, 55.88; H, 6.74; N, 18.33. Found: C, 55.36; H, 6.88; N, 18.04%. APIES-MS (fragments are based on ^{35}Cl, Ir%): *m*/z 690 ($[M]^+$, 100). FTIR (KBr, cm^{-1}): 3082, 3039 (C–H arom.), 1058 (C–F), 1212, 1186 (P=N).

*2.2.17. 7,10-Bis(4-fluorobenzyl)-2,2,4,4-tetramorpholin-4-yl-1,3,5,7,10-pentaaza-2λ^5,4λ^5,6λ^5-triphosphaspiro[4.5]dodeca-1,3,5-triene (**5c**)*

The procedure was similar to that of compound **1b**, using **5a** (1.14 g, 2.07 mmol), morpholine (2.17 mL, 25.00 mmol) and triethylamine (1.20 mL) (31 h). The product was purified by column chromatography using toluene-THF (1:1) and crystallized from *n*-heptane. Yield: 1.17 g (75%). M.p.: 260 °C. *Anal.* Calc. for $C_{32}H_{48}N_9F_2P_3O_4$: C, 51.03; H, 6.42; N, 16.73. Found: C, 51.48; H, 6.06; N, 16.37%. APIES-MS (fragments are based on ^{35}Cl, Ir%): *m*/z 754 ($[MH]^+$, 100). FTIR (KBr, cm^{-1}): 3070, 3020 (C–H arom.), 1054 (C–F), 1224, 1190 (P=N).

*2.2.18. 7,10-Bis(4-fluorobenzyl)-2,2,4,4-tetra-1,4-dioxa-8-azaspiro[4.5]dec-8-yl-1,3,5,7,10-pentaaza-2λ^5,4λ^{5}69λ^5-triphosphaspiro[4.5]dodeca-1,3,5-triene (**5d**)*

The procedure was similar to that of compound **1b**, using **5a** (1.08 g, 1.96 mmol), DASD (3.00 mL, 24.00 mmol) and triethylamine (1.10 mL) (31 h). The product was purified by column chromatography using toluene-THF (3:1) and crystallized from *n*-heptane. Yield: 1.17 g (75%). M.p.: 300 °C. *Anal.* Calc. for $C_{44}H_{64}N_9F_2P_3O_8$: C, 54.04; H, 6.60; N, 12.89. Found: C, 54.87; H, 6.39; N, 12.42%. APIES-MS (fragments are based on ^{35}Cl, Ir%): *m*/z 978 ($[M]^+$, 100). FTIR (KBr, cm^{-1}): 3073, 3046 (C–H arom.), 1051 (C–F), 1215, 1198 (P=N).

2.3. X-ray crystallography

Suitable crystals of compounds **3a**, **4a**, **5a** and **2b** were obtained from toluene at room temperature. The crystallographic data are given in Table 1, selected bond lengths and angles are listed in Table 2 and hydrogen bond data are given in Table 3. Crystallographic data were recorded on a Bruker Kappa APEXII CCD area-detector diffractometer using MoKα radiation (λ = 0.71073 Å) at *T* = 100(2) K. Absorption corrections by multi-scan [27] were applied. The structures were solved by direct methods and refined by full-matrix least squares against F^2 using all data [28]. All non-H atoms were refined anisotropically. In compounds **3a**, **4a**, **5a** and **2b**, the H atom positions were calculated geometrically at distances of 0.93 Å (CH) and 0.97 Å (CH_2) from the parent C atoms; a riding model was used during the refinement process and the U_{iso}(H) values were constrained to 1.2 U_{eq}(carrier atom).

Table 1
Crystallographic data for **3a**, **4a**, **5a** and **2b**.

	3a	**4a**	**5a**	**2b**
Empirical formula	$C_{18}H_{20}Cl_4F_2N_5P_3$	$C_{17}H_{18}Cl_4F_2N_5P_3$	$C_{16}H_{16}Cl_4F_2N_5P_3$	$C_{26}H_{45}FN_9P_3$
Formula weight	579.12	565.07	551.05	595.62
Crystal system	triclinic	monoclinic	monoclinic	triclinic
Space group	$P\bar{1}$	P 2_1/c	C 2/c	$P\bar{1}$
a (Å)	9.4049(2)	8.9912(2)	22.8721(7)	10.6000(2)
b (Å)	11.4354(3)	13.8214(3)	8.8214(3)	11.5826(2)
c (Å)	12.0907(4)	18.7501(4)	11.9577(4)	13.6823(3)
α (°)	106.658(3)	90.00	90.00	69.948(2)
β (°)	96.985(2)	98.111(4)	112.288(1)	75.185(3)
γ (°)	105.415(3)	90.00	90.00	75.152(3)
V (Å^3)	1173.08(6)	2306.78(9)	2232.38(13)	1499.05(6)
Z	2	4	4	2
μ (MoKα) (cm^{-1})	0.744 (MoKα)	0.754 (MoKα)	0.777 (MoKα)	0.238 (MoKα)
ρ (Calc.) (g cm^{-3})	1.640	1.627	1.640	1.320
Number of reflections total	21028	19380	7903	25799
Number of reflections unique	5844	5596	2540	7405
R_{int}	0.0230	0.0485	0.0201	0.0200
$2\theta_{max}$ (°)	56.76	57.18	55.12	56.80
T_{min}/T_{max}	0.7940/0.8534	0.7782/0.7943	0.6973/0.9263	0.9066/0.9429
Number of parameters	289	280	137	352
R [$F^2 > 2\sigma(F^2)$]	0.0261	0.0447	0.0238	0.0389
wR	0.0690	0.1153	0.0637	0.1026

Table 2
The selected bond lengths (Å) and angles (°) with the selected torsion angles (°) for **3a**, **4a**, **5a** and **2b**.

3a		4a		5a		2b	
P1–N1	1.615(2)	P1–N1	1.607(2)	P1–N1	1.616(0)	P1–N1	1.529(2)
P1–N3	1.619(1)	P1–N3	1.631(2)	P1–N1′	1.617(0)	P1–N3	1.592(2)
P1–N4	1.631(1)	P1–N4	1.642(2)	P1–N3	1.629(0)	P1–N4	1.687(1)
P1–N5	1.629(1)	P1–N5	1.629(2)	P1–N3′	1.629(0)	P1–N5	1.663(1)
P2–N1	1.561(1)	P2–N1	1.560(2)	P2–N1	1.563(1)	P2–N1	1.611(1)
P2–N2	1.588(1)	P2–N2	1.591(2)	P2–N2	1.584(0)	P2–N2	1.592(2)
P3–N3	1.559(1)	P3–N3	1.556(2)	P2′–N2	1.584(0)	P3–N3	1.595(1)
P3–N2	1.587(2)	P3–N2	1.588(2)	P2′–N1′	1.563(1)	P3–N2	1.600(2)
P2–Cl2	1.997(6)	P2–Cl2	1.994(10)	P2–Cl1	1.994(1)	P2–N7	1.653(2)
P3–Cl4	2.013(5)	P3–Cl4	2.022(8)	P2–Cl2	2.013(1)	P3–N9	1.657(2)
N1–P1–N3	113.2(1)	N1–P1–N3	111.0(1)	N1–P1–N3	115.2(0)	N1–P1–N3	118.3(1)
N1–P1–N4	115.3(1)	N1–P1–N4	109.1(1)	N1′–P1–N3	109.8(0)	N1–P1–N4	107.8(1)
N1–P1–N5	106.5(1)	N1–P1–N5	109.8(1)	N3′–P1–N1	109.8(0)	N1–P1–N5	110.6(1)
N3–P1–N4	105.5(1)	N3–P1–N4	110.4(1)	N3′–P1–N1′	115.2(0)	N3–P1–N4	109.2(1)
N3–P1–N5	113.5(1)	N3–P1–N5	112.0(1)	N3–P1–N3′	94.7(0)	N3–P1–N5	107.4(1)
N4–P1–N5	102.6(1)	N4–P1–N5	104.2(1)	N1–P1–N1′	111.4(0)	N4–P1–N5	102.4(1)
N1–P2–N2	119.7(1)	N1–P2–N2	120.1(1)	N1–P2–N2	119.6(0)	N1–P2–N2	116.6(1)
N3–P3–N2	120.2(1)	N3–P3–N2	119.5(1)	P2–N2–P2′	118.3(0)	N3–P3–N2	115.2(1)
N3–P1–N1–P2	–1.0(1)	N3–P1–N1–P2	3.7(2)	N3–P1–N1–P2	–131.4(0)	N3–P1–N1–P2	7.3(1)
N4–P1–N1–P2	120.6(9)	N4–P1–N1–P2	125.6(2)	N3′–P1–N1–P2	123.3(0)	N4–P1–N1–P2	131.7(9)

Table 3
Hydrogen-bond geometry (,°).

Compound	D–H···A	D–H	H···A	D···A	D–H···A
3a	C6–H6A···N3	0.97	2.50	3.010 (2)	112.7(1)
	C17–H17A···N1	0.97	2.41	2.956 (2)	115.2(1)
4a	C2–H2···N3^{i}	0.93	2.44	3.366 (3)	177.4(2)
2b	C9–H92···N6^{ii}	0.99	2.55	3.544 (2)	177.7(1)
	C7–H71···N1	0.99	2.65	3.139 (2)	110.7(1)

Symmetry codes: $^{i}x - 1, y, z$; $^{ii}-x, -y + 1, -z$.

3. Results and discussion

3.1. Synthesis

The starting compounds, mono and bis(4-fluorobenzyl)diamines (**1**–**5**), were obtained from the reduction of the corresponding Schiff bases prepared from 4-fluorobenzaldehyde with the appropriate diamines in methanol. The reaction yields of the mono(4-fluorobenzyl)diamines (**1** and **2**) are higher than those of the bis(4-fluorobenzyl)diamines (**3** and **4**). The yield of **3** is very low. The reaction of 4-fluorobenzyaldehyde with ethylene diamine gave eventually only the bis product, *N*,*N*′-bis(4-fluorobenzyl)ethane-1,2-diamine (**5**), and the expected mono product, *N*-(4-fluorobenzyl)ethane-1,2-diamine, could not be obtained. The tetrachloromono(4-fluorobenzyl) monospirocyclophosphazene derivatives (**1a** and **2a**) and tetrachlorobis(4-fluorobenzyl) monospirocyclophosphazenes (**3a**–**5a**) have been synthesized from the reactions of $N_3P_3Cl_6$, with the mono (**1** and **2**) and bis(4-fluorobenzyl)diamines (**3**-**5**), respectively in dry THF. The amount of **3a** is very limited, which is why the reactions of **3a** with amines could not be carried out. All the fully substituted mono(4-fluorobenzyl) monospirocyclophosphazenes (**1b**–**2d**) and bis(4-fluorobenzyl) monospirocyclophosphazenes (**4b**, **4d**–**5d**) are prepared from the reactions of **1a**, **2a**, **4a** and **5a** with excess pyrrolidine, morpholine and DASD in boiling THF (Scheme 1). The chloride replacement reactions of $N_3P_3Cl_6$ with the bifunctional ligands **1**–**5** appear to be regioselective because only spirocyclic compounds are formed. On the other hand, the partly substituted phosphazenes

4e and **4f** have been obtained by the reactions of **4a** with excess morpholine and DASD respectively, in boiling THF. All attempts for the preparation of the expected fully substituted products **4c** and **4d** failed in boiling THF, while compound **4d** has been prepared in boiling o-xylene. All the new phosphazenes have been purified by column chromatography.

The microanalyses, FTIR, APIES-MS and NMR data are in agreement with the proposed structures of the compounds. In addition, the mass spectra of all the compounds display the molecular [M^+] ion peaks.

3.2. NMR and FTIR spectroscopy

The ^{1}H decoupled ^{31}P NMR data of all the compounds indicate that they have monospirocyclic structures. The spin systems are interpreted as simple AB_2 for **1c**, **1d**, **2b**, **2c**, **2d** and **4d**, AX_2 for **1a**–**5a**, **1b**, **4b**, **5b**, **5c** and **5d**, and ABX for **4e** and **4f**. The coupling constants $^2J_{PP}$ of the compounds are in the range 36.9–47.9 Hz. The average value of $^2J_{PP}$ is 41.5 Hz. As expected, compounds **1a**–**5a**, **1b**, **4b**, **5b**, **5c** and **5d** give rise to one triplet and one doublet in the ^{1}H decoupled ^{31}P NMR spectra. This finding is clearly in agreement with the two different kinds of P atoms present in the cyclophosphazene skeleton. While, in **4e** and **4f** three different kinds of P atoms are present, according to their ^{31}P NMR data (Table 4).

The ^{1}H and ^{13}C NMR signals of all the phosphazenes are assigned on the basis of chemical shifts, multiplicities and chemical constants. The assignments are made undoubtedly using HSQC and HMBC experiments (Tables 5 and 6). As an example, the HSQC and HMBC spectra of **1d** are illustrated in the Supplementary material (Figs. S1a and S1b). The benzylic ArCH_2N protons of all the compounds are observed at 3.84–4.37 ppm, and give rise to doublets, indicating that these protons are equivalent to each other. The $^3J_{PH}$ coupling constants of the tetrachloro (**1a**–**5a**) and seven-membered fully substituted spiro cyclic phosphazenes (**1b**, **1c** and **1d**) are larger than those of the five and six-membered ones (Table 5). On the other hand, the assignments of the aromatic protons are also clearly made using the coupling constants of $^3J_{FH}$ and $^4J_{FH}$. As expected, the average values of $^3J_{FH}$ and $^4J_{FH}$ are 8.6 and 5.5 Hz, respectively. The protons (H_3 and H_5) and (H_2 and H_6) are observed at ca. 7.38 and 7.02 ppm, respectively, as two groups of multiplets for all the compounds except **1d**, **4e** and **4f**. In the ^{1}H NMR spectra of the partly substituted bis-(4fluorobenzyl) monospirocyclophosphazenes (**4e** and **4f**), the two substituents bonded to the same P atoms show two groups of NCH_2 and NCH_2CH_2 signals with small separations (Table 5).

As expected, in $CDCl_3$ solution all of the bis(4-fluorobenzyl) monospirocyclophosphazenes have symmetric structures, according to their ^{1}H and ^{13}C NMR spectral data. In the ^{13}C NMR spectra of all the compounds, the expected carbon signals are assigned. The NCH_2 signals of the compounds are determined using HSQC and HMBC experiments, and these are observed at 46.21–46.34 ppm for NCH_2(pyrr), 43.79–44.80 ppm for NCH_2 (morph), 42.53–42.72 ppm for NCH_2 (DASD), 47.83–51.67 ppm for ArCH_2N, 44.23–47.05 ppm for NCH_2 and 40.05–41.77 ppm for NHCH_2. The $^3J_{PC}$ couplings give rise to triplets for the NCH$_2$CH_2(pyrr) carbons of **1b**, the NCH$_2$CH_2(pyrr) carbons of **5b**, and the OCH_2(morph) carbons of **5c** (Supplementary material, Fig. S2). The triplets probably depend on the second-order effects that were previously observed for some phosphazene compounds [2] and the $^3J_{PC}$ coupling constants are estimated using the external transitions of the triplets [29]. In addition, the $^3J_{PC}$ couplings of the ipso-C_4 carbons and P atoms are observed at 4.9–10.9 Hz, and the average value is 7.6 Hz. On the other hand, the $^3J_{PC}$ values of compounds containing seven-membered spiro-rings (**1a**, **3a**, **1b**, **1c** and **1d**) are smaller than those containing five- and six-membered spiro-rings. In addition, the assignments of the aromatic carbons are easily determined using the coupling constants of $^1J_{FC}$, $^2J_{FC}$, $^3J_{FC}$ and $^4J_{FC}$. As expected, the average values of $^1J_{FC}$, $^2J_{FC}$, $^3J_{FC}$ and $^4J_{FC}$ are 245.1, 21.4, 8.3 and 2.8 Hz, respectively.

The ^{19}F NMR spectra of **1d** and **2d** are recorded as examples, and the chemical shifts values are observed at −117.02 and −116.56 ppm, respectively.

The characteristic C–F stretching vibrations are strongly coupled with the C–H in-plane bending vibrations in the mono fluorinated benzene and are observed at 1100–1000 cm^{-1} [30]. The ν_{C-F} values are in agreement with the literature findings. All the phosphazene derivatives show two medium intensity absorption bands at 3082–3053 and 3048–3020 cm^{-1}, attributed to the asymmetric and symmetric stretching vibrations of the Ar–H protons. The phosphazene derivatives also display intense bands between 1236 and 1172 cm^{-1}, related to the $\nu_{P=N}$ bonds of the phosphazene ring [31,32]. The characteristic ν_{NH} stretching vibrations of the mono(4-fluorobenzyl) monospirocyclophosphazenes (**1a**, **2a**,**1b**–**2d**) are observed at 3398–3242 cm^{-1}. In addition, asymmetric and symmetric vibrations of ν_{PCl2} have arisen for the partly substituted spirocyclophosphazenes (**1a**–**5a**) at 579–568 and 518–510 cm^{-1}.

Table 4
^{31}P NMR data in $CDCl_3$ (δ in ppm, J in Hz).

Compound	Spin system	δPN (spiro)	δPCl$_2$	δPN$_2$	δPNCl	$^2J_{PP}$
1a	AX_2	P_A: 14.40	P_X: 21.10	–	–	$^2J_{AX}$: 45.7
2a	AX_2	P_A: 10.38	P_X: 22.17	–	–	$^2J_{AX}$: 41.3
3a	AX_2	P_A: 16.33	P_X: 20.94	–	–	$^2J_{AX}$: 45.3
4a	AX_2	P_A: 12.70	P_X: 22.60	–	–	$^2J_{AX}$: 38.4
5a	AX_2	P_A: 18.00	P_X: 24.20	–	–	$^2J_{AX}$: 42.9
1b	AX_2	P_A: 22.25	–	P_X: 18.50	–	$^2J_{AX}$: 42.1
2b	AB_2	P_A: 20.56	–	P_B: 18.71	–	$^2J_{AB}$: 36.9
4b	AX_2	P_A: 23.59	–	P_X: 17.84	–	$^2J_{AX}$: 39.2
5b	AX_2	P_A: 27.75	–	P_X: 18.64	–	$^2J_{AX}$: 43.0
1c	AB_2	P_A: 22.54	–	P_B: 21.72	–	$^2J_{AB}$: 43.9
2c	AB_2	P_A: 19.97	–	P_B: 21.06	–	$^2J_{AB}$: 38.3
5c	AX_2	P_A: 28.14	–	P_X: 22.17	–	$^2J_{AX}$: 42.5
1d	AB_2	P_A: 21.95	–	P_B: 21.48	–	$^2J_{AB}$: 38.0
2d	AB_2	P_A: 19.55	–	P_B: 20.76	–	$^2J_{AB}$: 40.9
4d	AB_2	P_A: 22.44	–	P_B: 20.27	–	$^2J_{AB}$: 39.9
5d	AX_2	P_A: 27.87	–	P_X:22.13	–	$^2J_{AX}$: 43.1
4e	ABX	P_A: 19.55	P_X: 31.15	–	P_B: 20.01	$^2J_{AX}$: 41.4 $^2J_{AB}$: 39.4 $^2J_{BX}$: 47.9
4f	ABX	P_A: 19.31	P_X: 30.83	–	P_B: 20.00	$^2J_{AX}$: 43.0 $^2J_{AB}$: 38.7 $^2J_{BX}$: 41.3

Table 5
^{1}H NMR data for the compounds [δ are reported in ppm, J values in Hz, *d*: DASD, *m*: morpholine, *p*: pyrrolidine, s: singlet, d: doublet, t: triplet, q: quartet and m: multiplet].

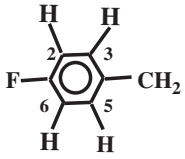	***H*$_2$, *H*$_6$**	***H*$_3$, *H*$_5$**	N–CH$_2$–C***H*$_2$**	NH–CH$_2$–C***H*$_2$**	N–C***H*$_2$**	NH–C***H*$_2$**	Ar–C***H*$_2$**–N	O–C***H*$_2$**	N***H***
1a	7.00 $^3J_{HH}$ = 8.5 $^3J_{FH}$ = 8.6	7.30 $^3J_{HH}$ = 8.5 $^4J_{FH}$ = 5.5	1.50(m,2H)	1.65(m,2H)	3.20(m,3H)	3,10(m,1H)	4.30(d,2H) $^3J_{PH}$ = 13.1	–	2.50(m,1H)
2a	7.05 $^3J_{HH}$ = 8.6 $^3J_{FH}$ = 8.7	7.38 $^3J_{HH}$ = 8.6 $^4J_{FH}$ = 5.4	1.78(m,2H)	–	3.31(m,2H)	3.05(m,2H)	3.97(d,2H) $^3J_{PH}$ = 9.2	–	2.87(m,1H)
3a	7.05 $^3J_{HH}$ = 8.6 $^3J_{FH}$ = 9.8	7.34 $^3J_{HH}$ = 8.6 $^4J_{FH}$ = 5.2	1.53(m,4H)	–	3.27(d,4H) $^3J_{PH}$ = 15.6	–	4.37(d,4H) $^3J_{PH}$ = 13.5	–	–
4a	7.07 $^3J_{HH}$ = 8.4 $^3J_{FH}$ = 8.6	7.41 $^3J_{HH}$ = 8.4 $^4J_{FH}$ = 5.5	1.76(m,2H)	–	3.05(m,4H) $^3J_{PH}$ = 14.2 $^3J_{HH}$ = 8.1	–	4.05(d,4H) $^3J_{PH}$ = 9.4	–	–
5a	7.10 $^3J_{HH}$ = 8.2 $^3J_{FH}$ = 8.6	7.40 $^3J_{HH}$ = 8.2 $^4J_{FH}$ = 5.5	–	–	3.12(d,4H) $^3J_{PH}$ = 10.3	–	4.10(d,4H) $^3J_{PH}$ = 9.6	–	–
1b	6.90 $^3J_{HH}$ = 8.4 $^3J_{FH}$ = 8.7	7.40 $^3J_{HH}$ = 8.4 $^4J_{FH}$ = 5.6	1.40(m,2H) *p*:1.65(m,8H) 1.74(m,8H)	1.50(m,2H)	3.08(m,2H) *p*:3.08(m,16H)	2.95(m,2H)	4.30(d,2H) $^3J_{PH}$ = 11.1	–	2.48(m,1H)
2b	6.97 $^3J_{HH}$ = 8.6 $^3J_{FH}$ = 8.7	7.38 $^3J_{HH}$ = 8.6 $^4J_{FH}$ = 5.6	1.61(m,2H) *p*:1.75(m,16H)	–	3.10(m,2H) *p*:3.18(m,16H)	2.91(m,2H) $^3J_{PH}$ = 13.4	3.91(d,2H) $^3J_{PH}$ = 6.8	–	2.38(m,1H)
4b	7.00 $^3J_{HH}$ = 8.5 $^3J_{FH}$ = 8.7	7.40 $^3J_{HH}$ = 8.5 $^4J_{FH}$ = 5.6	1.64(m,2H) *p*:1.73(m,16H)	–	3.00(m,4H) $^3J_{PH}$ = 13.9 $^2J_{HH}$ = 8.2 *p*:3.15(m,16H)	–	4.10(d,4H) $^3J_{PH}$ = 6.7	–	–
5b	7.00 $^3J_{HH}$ = 8.4 $^3J_{FH}$ = 8.7	7.43 $^3J_{HH}$ = 8.4 $^4J_{FH}$ = 5.6	*p*:1.74(m,16H)	–	2.95(d,4H) $^3J_{PH}$ = 10.0 *p*: 3.15(m,16H)	–	4.01(d,4H) $^3J_{PH}$ = 6.6	–	–
1c	6.99 $^3J_{HH}$ = 8.5 $^3J_{FH}$ = 8.7	7.42 $^3J_{HH}$ = 8.5 $^4J_{FH}$ = 5.5	1.38(m,2H)	1.52(m,2H)	3.10 (m,2H) *m*:3.15(m,16H)	3.05(m,2H)	4.25(d,2H) $^3J_{PH}$ = 9.3	*m*:3.55(t,8H) 3.65(t,8H) $^3J_{HH}$ = 4.4 $^3J_{HH}$ = 4.5	2.40(m,1H)
2c	7.01 $^3J_{HH}$ = 8.5 $^3J_{FH}$ = 8.7	7.36 $^3J_{HH}$ = 8.5 $^4J_{FH}$ = 5.9	1.65(m,2H)	–	3.20(m,2H) *m*:3.24(m,16H)	2.94(m,2H) $^3J_{PH}$ = 13.7	3.87(d,2H) $^3J_{PH}$ = 6.5	*m*:3.59(m,16H)	2.28(m,1H)
5c	7.04 $^3J_{HH}$ = 8.6 $^3J_{FH}$ = 8.7	7.37 $^3J_{HH}$ = 8.6 $^4J_{FH}$ = 5.4	–	–	3.03(d,4H) $^3J_{PH}$ = 10.2 *m*:3.17(m,16H)	–	4.01(d,4H) $^3J_{PH}$ = 6.6	*m*:3.64(m,16H)	–
1d	7.00; 7.18 $^3J_{HH}$ = 8.3; 8.4 $^3J_{FH}$ = 8.7; 8.8	7.43; 7.26 $^3J_{HH}$ = 8.3; 8.4 $^4J_{FH}$ = 5.7; 5,8	1.52(m,2H) *d*:1.66(m,8H) 1.69(m,8H)	1.57(m,2H)	3.11(m,2H) *d*:3.17(m,8H) 3.21(m,8H)	2.85(m,2H)	4.26(d,2H) $^3J_{PH}$ = 9.0	*d*:3.91(m,8H) 3.96(m,8H)	1.69(m,1H)
2d	6.99 $^3J_{HH}$ = 8.5 $^3J_{FH}$ = 8.7	7.37 $^3J_{HH}$ = 8.5 $^4J_{FH}$ = 5.6	1.69(m,2H) *d*:1.60(m,16H)	–	3.05(m,2H) *d*:3.22(m,16H)	2.92(m,2H) $^3J_{PH}$ = 11.5 $^3J_{HH}$ = 5.8	3.84(d,2H) $^3J_{PH}$ = 6.8	*d*:3.93(m,8H) 3.96(m,8H)	1.79(m,1H)
4d	6.97 $^3J_{HH}$ = 8.3 $^3J_{FH}$ = 8.6	7.35 $^3J_{HH}$ = 8.4 $^4J_{FH}$ = 5.5	1.61(m,2H) *d*:1.53(m,16H)	–	2.95(m,4H) $^3J_{PH}$ = 13.8 $^2J_{HH}$ = 8.1 *d*:3.14(m,16H)	–	3.96(d,4H) $^3J_{PH}$ = 6.7	*d*:3.88(m,16H)	–
5d	7.02 $^3J_{HH}$ = 8.2 $^3J_{FH}$ = 8.3	7.38 $^3J_{HH}$ = 8.2 $^4J_{FH}$ = 5.6	*d*:1.60(m,16H)	–	2.99(d,4H) $^3J_{PH}$ = 9.9 *d*:3.24(m,16H)	–	4.01(d,4H) $^3J_{PH}$ = 6.0	*d*:3.88(m,16H)	–
4e	7.01; 7.04 $^3J_{HH}$ = 8.5; 8.4 $^3J_{FH}$ = 8.7; 8.6	7.37; 7.44 $^3J_{HH}$ = 8.5; 8.4 $^4J_{FH}$ = 5.4; 5.4	1.70(m,2H)	–	2.95(m,4H) *m*:3.10(m,8H) 3.20(m,4H)	–	3,96(d,2H) $^3J_{PH}$ = 7.9 3,90(d,2H) $^3J_{PH}$ = 8.0	*m*:3.55(m,8H) 3.62(m,4H)	–
4f	7.02; 7.05 $^3J_{HH}$ = 8.5; 8.6 $^3J_{FH}$ = 8.7; 8.8	7.37; 7.42 $^3J_{HH}$ = 8.5; 8.6 $^4J_{FH}$ = 5.4; 5.5	1.59(m,2H) *d*:1.60(m,8H) 1.66(m,4H)	–	2.83(m,4H) *d*: 3.13(m,8H) 3.15(m,4H)	–	4.05(d,2H) $^3J_{PH}$ = 8.6 4.15(d,2H) $^3J_{PH}$ = 8.8	*d*:3.84(m,8H) 3.83(m,4H)	–

3.3. X-ray structures of ***3a***, ***4a***, *5a* and ***2b***

The molecular and solid-state structure determinations of **3a**, **4a**, **5a** and **2b** confirm the assignments of their structures from spectroscopic data. The molecular structures of **3a**, **4a**, **5a** and **2b**, along with the atom numbering schemes, are depicted in Figs. 1–4, respectively. The phosphazene rings of **3a**, **4a** and **2b** are in flattened-boat conformations [Supplementary material, Fig. S3a; $\varphi_2 = -26.4(4)^\circ$, $\theta_2 = 108.4(4)^\circ$, Fig. S4a; $\varphi_2 = -151.9(6)^\circ$, $\theta_2 = 60.7(5)^\circ$, and Fig. S5a; $\varphi_2 = 6.2(1.3)^\circ$, $\theta_2 = 157.0(5)^\circ$] having total

Table 6
^{13}C NMR (decoupled) spectral data for the compounds [δ are reported in ppm, J values in Hz, *d*: DASD, *m*: morpholine and *p*: pyrrolidine].

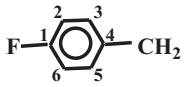	C_4	C_3, C_5	C_2, C_6	C_1	N–CH_2–CH_2	NH–CH_2–CH_2	N–CH_2	NH–CH_2	Ar–CH_2–N	O–CH_2	O–C–O
1a	134.12 $^3J_{PC}$ = 6.0	129.33 $^3J_{FC}$ = 7.9	115.41 $^2J_{FC}$ = 21.5	162.13 $^1J_{FC}$ = 245.2	27.36	31.10	45.92 $^2J_{PC}$ = 7.1	40.50	50.77 $^2J_{PC}$ = 6.1	–	–
2a	132.20 $^3J_{PC}$ = 8.9	129.57 $^3J_{FC}$ = 8.0	114.91 $^2J_{FC}$ = 21.4	161.85 $^1J_{FC}$ = 246.0	26.00 $^3J_{PC}$ = 4.5	–	45.55 $^2J_{PC}$ = 3.4	40.35	49.75 $^2J_{PC}$ = 3.0	–	–
3a	134.06 $^3J_{PC}$ = 4.9	129.14 $^3J_{FC}$ = 7.9	115.46 $^2J_{FC}$ = 21.4	162.15 $^1J_{FC}$ = 245.2	26.27	–	45.12 $^2J_{PC}$ = 6.7	–	50.20 $^2J_{PC}$ = 6.8	–	–
4a	132.52 $^3J_{PC}$ = 8.2	130.01 $^3J_{FC}$ = 8.1	115.46 $^2J_{FC}$ = 21.3	162.39 $^1J_{FC}$ = 245.9	25.16	–	45.77	–	50.14 $^2J_{PC}$ = 3.7	–	–
5a	132.33 $^3J_{PC}$ = 9.1	129.94 $^3J_{FC}$ = 8.1	115.56 $^2J_{FC}$ = 21.5	162.42 $^1J_{FC}$ = 245.8	–	–	44.23 $^2J_{PC}$ = 14.6	–	47.83 $^2J_{PC}$ = 6.0	–	–
1b	136.70 $^3J_{PC}$ = 5.0	129.27 $^3J_{FC}$ = 7.9	114.52 $^2J_{FC}$ = 21.2	161.61 $^1J_{FC}$ = 243.4	27.90 *p*: 26.37 26.26 $^3J_{PC}$ = 9.2 $^3J_{PC}$ = 9.8	32.05	45.54 $^2J_{PC}$ = 6.6 *p*: 46.25 46.34 $^2J_{PC}$ = 2.0	40.05	51.01 $^2J_{PC}$ = 5.5	–	–
2b	135.04 $^3J_{PC}$ = 10.6 $^4J_{FC}$ = 3.0	130.03 $^3J_{FC}$ = 7.8	114.71 $^2J_{FC}$ = 21.2	161.80 $^1J_{FC}$ = 244.2	28.33 *p*: 26.26 26.31 $^3J_{PC}$ = 9.5 $^3J_{PC}$ = 9.4	–	46.77 *p*: 46.06 46.21	41.77	51.12 $^2J_{PC}$ = 1.0	–	–
4b	135.40 $^3J_{PC}$ = 10.9 $^4J_{FC}$ = 3.0	129.51 $^3J_{FC}$ = 7.8	114.68 $^2J_{FC}$ = 21.2	161.81 $^1J_{FC}$ = 243.9	26.31 $^3J_{PC}$ = 9.2 *p*: 23.97	–	45.98 *p*: 46.28	–	50.25 $^2J_{PC}$ = 1.7	–	–
5b	134.86 $^3J_{PC}$ = 8.8 $^4J_{FC}$ = 2.6	129.54 $^3J_{FC}$ = 7.9	114.95 $^2J_{FC}$ = 21.2	161.94 $^1J_{FC}$ = 244.4	*p*: 26.30 $^3J_{PC}$ = 9.5	–	44.23 $^2J_{PC}$ = 11.5 *p*: 46.23	–	48.79 $^2J_{PC}$ = 5.7	–	–
1c	136.21 $^3J_{PC}$ = 6.5	129.54 $^3J_{FC}$ = 7.7	114.97 $^2J_{FC}$ = 21.2	161.89 $^1J_{FC}$ = 244.5	29.67	30.31	46.47 $^2J_{PC}$ = 6.6 *m*: 44.70 44.80	40.21	51.67 $^2J_{PC}$ = 5.2	*m*: 67.30 67.35 $^3J_{PC}$ = 7.8 $^3J_{PC}$ = 7.9	–
2c	134.15 $^3J_{PC}$ = 8.7	129.74 $^3J_{FC}$ = 7.9	115.09 $^2J_{FC}$ = 21.3	162.00 $^1J_{FC}$ = 244.9	28.17 $^3J_{PC}$ = 4.6	–	46.93 *m*: 44.75 $^2J_{PC}$ = 4.9	41.70 $^2J_{PC}$ = 2.7	51.19 $^2J_{PC}$ = 0.9	*m*: 67.21 $^3J_{PC}$ = 8.1	–
5c	133.88 $^3J_{PC}$ = 8.6	129.07 $^3J_{FC}$ = 7.9	115.33 $^2J_{FC}$ = 21.5	161.20 $^1J_{FC}$ = 246.2	–	–	44.51 $^2J_{PC}$ = 12.0 *m*: 44.77	–	48.91 $^2J_{PC}$ = 6.1	*m*: 67.26 $^3J_{PC}$ = 8.7	–
1d	136.49 $^3J_{PC}$ = 7.1	128.56 $^3J_{FC}$ = 7.7	114.79 $^2J_{FC}$ = 21.2	161.69 $^1J_{FC}$ = 243.2	28.34 *d*: 35.54	31.94	46.28 $^2J_{PC}$ = 5.9 d: 42.56 ;42.67	40.21	51.38 $^2J_{PC}$ = 5.4	*d*: 64.08 64.13	107.54 107.77
2d	134.49 $^3J_{PC}$ = 8.4	129.93 $^3J_{FC}$ = 7.9	114.86 $^2J_{FC}$ = 21.3	161.89 $^1J_{FC}$ = 244.1	28.25 $^3J_{PC}$ = 3.8 *d*: 35.56	32.50	47.05 $^2J_{PC}$ = 6.6 d: 42.69	41.75	51.56 $^2J_{PC}$ = 1.1	*d*: 64.16 64.32	107.58 107.79
4d	134.93 $^3J_{PC}$ = 8.5	129.51 $^3J_{FC}$ = 7.8	115.03 $^2J_{FC}$ = 21.2	161.94 $^1J_{FC}$ = 244.8	24.56 *d*: 35.70	–	46.32 d: 42.84	–	50.32 $^2J_{PC}$ = 1.2	*d*: 64.24	107.65
5d	134.30 $^3J_{PC}$ = 9.5	129.36 $^3J_{FC}$ = 7.9	115.10 $^2J_{FC}$ = 21.3	162.00 $^1J_{FC}$ = 244.4	*d*: 29.70	–	44.42 $^2J_{PC}$ = 11.5 *d*: 42.70	–	48.90 $^2J_{PC}$ = 5.0	*d*: 64.21	107.5
4e	133.55 133.70 $^3J_{PC}$ = 8.2 $^4J_{FC}$ = 2.6	129.37 128.75 $^3J_{FC}$ = 7.9 $^3J_{FC}$ = 7.8	114.83 114.61 $^2J_{FC}$ = 21.5 $^2J_{FC}$ = 21.6	161.63 161.61 $^1J_{FC}$ = 249.9 $^1J_{FC}$ = 241.7	24.29	–	45.80;45.25 *m*:44.15 43.79 $^2J_{PC}$ = 5.3 $^2J_{PC}$ = 2.6	–	49.87;49.76 $^2J_{PC}$ = 2,3 $^2J_{PC}$ = 2,4	*m*: 66.01 66.58 $^3J_{PC}$ = 11.9 $^3J_{PC}$ = 12.3	–
4f	134.39 $^3J_{PC}$ = 9.2 $^4J_{FC}$ = 2.7	130.30 129.70 $^3J_{FC}$ = 7.9 $^3J_{FC}$ = 7.9	114.94 115.08 $^2J_{FC}$ = 21.4 $^2J_{FC}$ = 21.5	162.03 $^1J_{FC}$ = 249.3	24.95 $^3J_{PC}$ = 4.8 *d*:34.68 $^3J_{PC}$ = 11.4 35.36 $^3J_{PC}$ = 11.6	–	45.77;46.21 *d*:42.53 42.72 $^2J_{PC}$ = 5.7 $^2J_{PC}$ = 2.6	–	50.10;50.32 $^2J_{PC}$ = 2.6 $^2J_{PC}$ = 2.7	*d*: 64.24	107.04 $^4J_{PC}$ = 1.7 107.46 $^4J_{PC}$ = 4.5

puckering amplitudes Q_T of 0.144(1) for **3a**, 0.174(2) for **4a** and 0.115(1) for **2b**. The phosphazene ring of **5a** is in a twisted conformation [Supplementary material, Fig. S6a; φ_2 = 90.0(0)°, θ_2 = 90.1(0)°] having total puckering amplitude Q_T of 0.123(0). In **4a** and **2b**, the six-membered rings (P1/N4/N5/C8-C10) are in chair conformations [Supplementary material, Fig. S4b; Q_T = 0.657(5) Å, φ_2 = −167.5(8)°, θ_2 = 38.2(2)°, Fig. S5b; Q_T = 1.188(3) Å, φ_2 = 143.9(2)°, θ_2 = 59.7(0.1)°] [33]. In **3a** and **5a**, the seven- and five-membered rings [(P1/N5/N4/C13-C16) and (P1/N3/N3′/C8/C8′)] are in twisted forms [Supplementary material, Fig. S3b; Q_T = 1.333(2) Å, φ_2 = 130.7(0.1)°, θ_2 = 50.5(0.1)°, Fig. S6b; φ_2 = −110.7(0)°]. As mentioned before in Section 3.2, in $CDCl_3$ solution **3a**, **4a** and **5a** have symmetric structures, according to their ^{1}H and ^{13}C NMR spectral data (Tables 5 and 6), but **3a** and **4a** are not symmetric structures in the solid state.

The average P–N bond lengths in the phosphazene rings of **3a**, **4a**, **5a** and **2b** are 1.588(1), 1.589(2), 1.588(1) and 1.597(1) Å, which are shorter than the spiro-ring P–N bonds of 1.631(1),

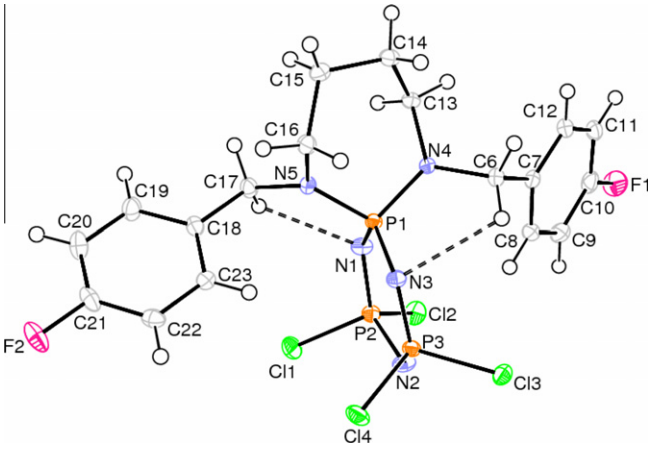

Fig. 1. An ORTEP-3 [34] drawing of **3a** with the atom numbering scheme. Displacement ellipsoids are drawn at the 30% probability level. Hydrogen bonds are shown as dashed lines.

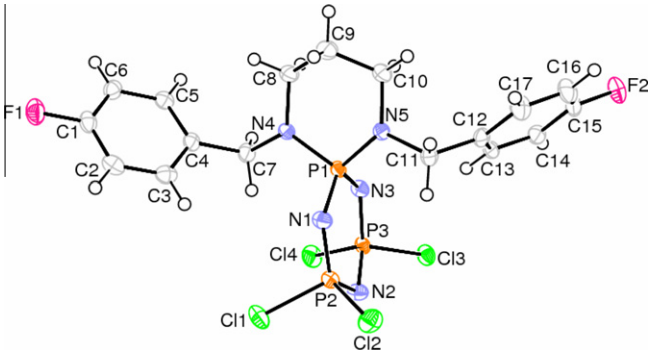

Fig. 2. An ORTEP-3 [34] drawing of **4a** with the atom numbering scheme. Displacement ellipsoids are drawn at the 30% probability level.

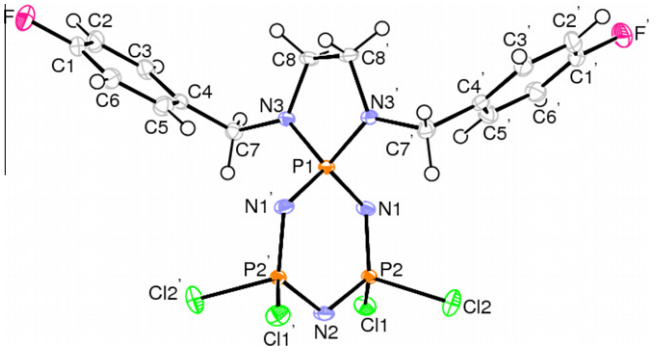

Fig. 3. An ORTEP-3 [34] drawing of **5a** with the atom numbering scheme. Displacement ellipsoids are drawn at the 30% probability level.

1.636(2), 1.629(1) and 1.675(1) Å, respectively. It is found that the P–N single and double bonds of phosphazenes are generally spread in the ranges 1.628–1.691 Å and 1.571–1.604 Å, respectively [35]. The results obtained in this study are in agreement with these values (Table 2). The P–N bond is, on the other hand, known to be the most intriguing bond in chemistry. In recent years, the electronic structures and the P–N bonds of phosphazene derivatives have been reinvestigated using natural bond orbital (NBO) and topological electron density analyses [36]. The ionic bonding and negative hyperconjugation alternatives for phosphazenes are evaluated with the NBO method. It is understood from the estimations that

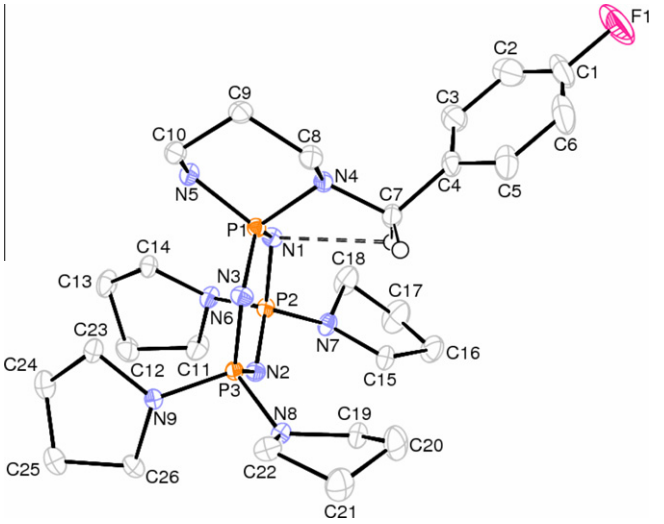

Fig. 4. An ORTEP-3 [34] drawing of **2b** with the atom numbering scheme. Displacement ellipsoids are drawn at the 30% probability level. Hydrogen bonds are shown as dashed lines.

ionic bonding is the dominant feature. Besides, these phosphazene bonding alternatives, in fact, are both very important and they are not mutually exclusive. The electron withdrawing groups bonding to the P atoms increase the negative hyperconjugation of the P–N bonds, and eventually contribute to the multiple-bond character. Thereby, an explanation for the shortening of the P–N bonds with electron withdrawing groups could be made qualitatively using more efficient π_N–α^*_{PR2} overlapping for the rings of the phosphazene derivatives [36,37].

The endocyclic N1–P1–N3 (α) and P2–N2–P3 (δ) angles of **3a**, **4a** and **5a** are narrowed, whilst the P1–N3–P3 (β) angles are highly expanded with respect to the corresponding values in the "standard" compound, $N_3P_3Cl_6$. In $N_3P_3Cl_6$, the α, β, γ and δ angles are 118.3(2), 121.4(3), 118.3(2) and 121.4(3)°, respectively [38]. On the other hand, in compound **2b**, the N3–P3–N2 (γ) angles [115.1(7) and 116.6(7)°] are narrowed, the β [123.1(8)°] and δ [123.9(8)°] angles are noticeably expanded, whereas the α [118.3(7)°] angle is unchanged. Generally, in phosphazenes the variations in the endocyclic and exocyclic angles may be explained by negative hyperconjugation and substituent-dependent charges at the P atoms. The charge separations between the N and P atoms in the phosphazenes differ significantly depending on the electron-withdrawing properties of the groups bonded to the P atoms [36]. Consequently, the electronic properties and the steric interactions of the substituents bonded to the P atoms of the phosphazenes can play an important role for the endocyclic and exocyclic angles, as their bond characters change [31].

In compound **2b**, there are both intramolecular C–H···N and intermolecular C–H···N hydrogen bonds (Table 3) (Fig. 4 and Supplementary material, Fig. S7), whilst in **3a** there are two intramolecular hydrogen bonds between the benzylic-CH protons and the nitrogen atoms of the phosphazene ring (Fig. 1). In addition, in **4a** intermolecular C–H···N hydrogen bonds link the molecules into infinite chains (Supplementary material, Fig. S8).

3.4. Antibacterial activity

The bacterial and fungal species used in this study were *Escherichia coli* (ATCC 35218), *E. coli* (ATCC 25922), *Staphylococcus aureus* (ATCC 6538), *Pseudomonas aerouginosa* (ATCC 27853), *Enterococcus faecalis* ATCC 292112, *Proteus vulgaris* (NRRL B-123), *B. cereus* (NRLL B-3008), *B. subtilis* (ATCC 29213), *C. albicans* (ATCC 10231) and *C. tropicalis* (ATCC 13803). Only the compounds **1b** and **4b** exhibit

Table 7
Antimicrobial activities of the compounds **1b** and **4b** (Antibiotics; Amp = Ampicilin and C = Chloramfenicol, Antifungal; Keto = Ketoconozole).

	Inhibition zone diameter (mm)				
	Agar well diffusion		Antibiotics	Antifungal	
Test bacteria/compounds	**1b**	**4b**	Amp	C	Keto
S. aureus ATCC 25923	15.00 ± 0.00	9.66 ± 0.57	35.0 ± 0.0	29.6 ± 0.5	NS
B. cereus NRRL-B-3711	16.66 ± 0.57	12.66 ± 0.57	10.0 ± 1.0	23.4 ± 0.7	NS
B. subtilis ATCC 6633	12.33 ± 0.57	11.33 ± 0.57	10.0 ± 1.0	23.4 ± 0.7	NS
C. albicans ATCC 10231	–	19.00 ± 0.00	NS	NS	30.0 ± 0.0
C. tropicalis ATCC 13803	–	25.00 ± 0.00	NS	NS	29.0 ± 0.5

Table 8
MIC Values of the compounds **1b** and **4b**.

	B. subtilis (μM)	*B. cereus* (μM)	*S. aureus* (μM)	*C. albicans*	*C. tropicalis*
1b	5000	5000	5000	–	–
4b	5000	5000	5000	312.5 μM	625 μM

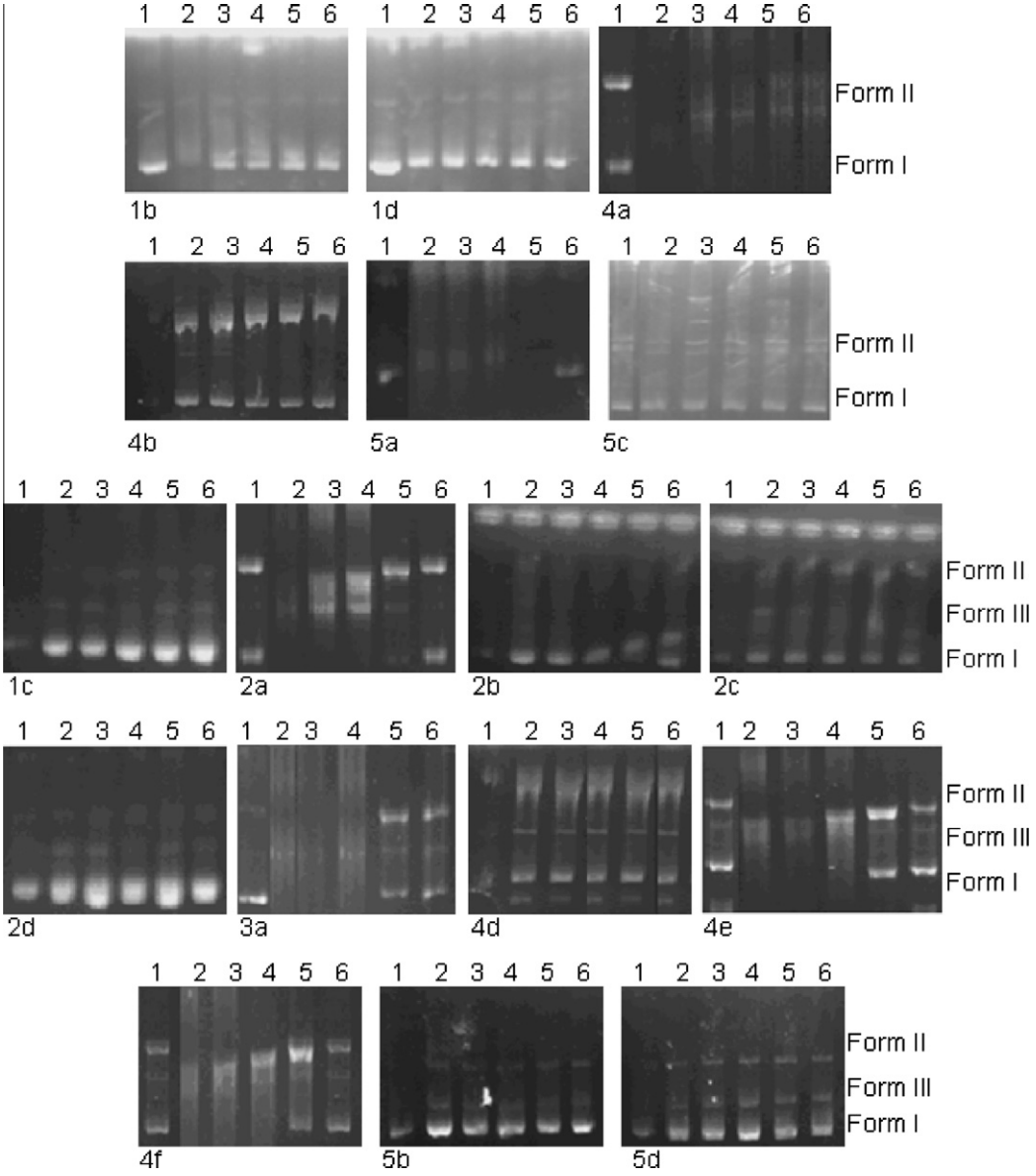

Fig. 5. Electrophoretic results of the incubation of pBR322 plasmid DNA with varying concentrations of **2a**–**5a**, **1b**–**2d**, **4b**, **4d**–**5d**, **4e** and **4f** (Lane 1): pBR322 DNA, Lanes 2–6: pBR322 DNA incubated with compounds 5.000, 2.500, 1.250, 625 and 312 μM. The roman numerals I and II indicate form I and form II and form III pBR322 plasmid DNAs respectively.

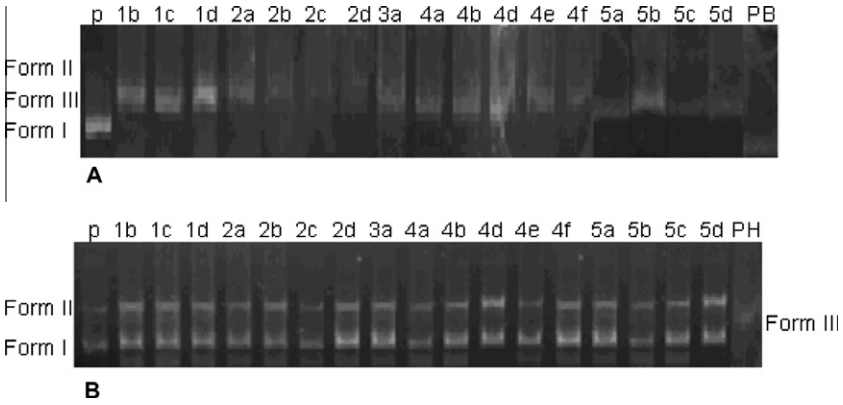

Fig. 6. Electrophoretograms for the *BamH*I (A) and *Hind*III (B) digested mixtures of pBR322 plasmid DNA after treatment with **1b**, **1c**, **1d**, **2a**, **2b**, **2c**, **2d**, **3a**, **4a**, **4b**, **4d**, **4e**, **4f**, **5a**, **5b**, **5c** and **5d**. Lane 1, untreated pBR322 plasmid DNA, line PB and PH apply to plasmid DNA restricted with enzymes *BamH*I and *Hind*III respectively.

antimicrobial activity against the bacterial and fungal species (Table 7). In addition, **1b** exhibits strong and moderate growth inhibition against *B. cereus*, *S. aureus* and *B. subtilis*. Compound **4b** is the only effective compound against the Cantida species. *C. albicans* and *C. tropicalis*. MIC values are in the range 312.5–5000 μM (Table 8).

3.5. Interactions of DNA with the compounds

Interactions of **2a**–**5a**, **1b**–**2d**, **4b**, **4d**–**5d**, **4e** and **4f** with supercoiled pBR322 plasmid DNA have been studied. The compounds were incubated over a range of concentrations with supercoiled pBR322 plasmid DNA in the dark at 37 °C for 24 h. The DNA cleavage by these compounds has been examined by observing the conversion of supercoiled DNA to the open circular form II and linear form III DNA. Fig. 5 depicts the electrophoretograms for the interaction of pBR322 plasmid DNA with the compounds **2a**–**5a**, **1b**–**2d**, **4b**, **4d**–**5d**, **4e** and **4f** at concentrations of the compounds ranging from 5000 to 312 μM. Lane 1 applies to the untreated pBR322 plasmid DNA (control DNA), showing the major supercoiled (form I) and minor nicked (form II) forms [2,23]. Lanes 2–6 apply to pBR322 plasmid DNA incubated with the compounds with concentrations ranging from 5000 to 312 μM.

When the pBR322 plasmid DNA interacted with decreasing concentrations of **1b**, **1d** and **5a**, the mobility of form I slightly decreased in all the concentrations tested. In the case of **4a**, the plasmid DNA interaction with the compound leads to a two strands break of the DNA, and the linear form III is observed. On the other hand, in the case of **4b**, **1c** and **2d**, the mobility of form I DNA increases and that of form II DNA decreases with a decreasing concentration of the compound. In addition, the linear form III DNA is generated with **1c**. Compounds **5c** and **2c** have no effect on the mobility of form I or form II DNA. However, these two compounds induce breaks in the DNA structure and form III is observed. Compounds **2a**, **3a**, **4f** and **4e** change the intensities and the mobilities of the form I DNA such that the two bands comigrate, especially at higher concentrations, and a smear of DNA is observed. In the case of **2b**, **5b** and **5d** there is no effect on the mobility of form I and form II DNA, however the linear form III bands are observed for **2b**, **5b** and **5d** as a result of conformational changes in form I of DNA emerging from covalent binding of the compounds with the nucleotides in DNA.

3.6. BamHI and HindIII digestion of compounds-pBR322 plasmid DNA

In order to find out whether the compounds bind guanine–guanine (GG) and/or adenine–adenine (AA) nucleotides of DNA, restriction analysis of the compound-DNA adducts digested with *BamH*I and *Hind*III enzymes was carried out. *BamH*I and *Hind*III enzymes bind at the sites DNA 5′-G/GATCC-3′ and 5′-A/AGCTT-3′ and cleave these sequences respectively, and convert forms I and II DNA to the linear form III DNA [39]. Only one concentration for each compound was used for the restriction analysis. All of the compounds prevent digestion with *Hind*III, whereas *BamH*I enzymes cut all the compounds interacted with DNA (Fig. 6).

4. Conclusions

The NN donor mono and bis(4-fluorobenzyl)diamines (**1–5**) have regioselectively led to the formation of spirocyclic mono (**1a** and **2a**) and bis(4-fluorobenzyl) monospirocyclophosphazenes (**3a–5a**) via chloride replacement reactions of $N_3P_3Cl_6$. The fully substituted mono(4-fluorobenzyl) (**1b–2d**) and bis(4-fluorobenzyl) (**4b**,**4d–5d**) monospirocyclophosphazenes are obtained from the reactions of compounds **1a–5a** with pyrrolidine, morpholine and DASD. Afterwards, the monochlorobis(4-fluorobenzyl) monospirocyclophosphazenes **4e** and **4f** have also been isolated from the reactions of excess morpholine and DASD in boiling THF. Compounds **4e** and **4f** have one stereogenic P atom and they can be thought of as good candidates for chiral investigations. The structures of the compounds have been ascertained unambiguously by one and two dimensional NMR techniques and X-ray crystallography. Especially, the assignments of the aromatic carbons are easily corroborated using the couplings between the fluorine and carbon atoms. The solid-state structures of **3a**, **4a**, **5a** and **2b** reveal intra and intermolecular C–H···N hydrogen bondings. Compounds **1b** and **4b** exhibit potential antimicrobial activities with Gram-positive bacteria. In addition, compound **4b** shows strong antifungal activities against *C. albicans* and *C. tropicalis.* Furthermore, the interactions of the compounds **2a**–**5a**, **1b**–**2d**, **4b**, **4d**–**5d**, **4e** and **4f** with pBR322 plasmid DNA have been evaluated. It is understood that they are very effective in changing the mobility and the shape of pBR322 plasmid DNA. Compounds **4a**, **5a**, **2a**, **3a**, **4e** and **4f** are the most efficient DNA cleavers amongst the other tested compounds. Moreover, restriction analyses indicate that phosphazene derivatives bind to A/T of the DNA.

Acknowledgements

The authors acknowledge the "Ankara University, Scientific Researches Unit" Grant No. 09B4240006, and also thank the "Medicinal Plants and Medicine Research Center of Anadolu University, Eskişehir" for the use of the X-ray facility. We also thank the State Planning Organization (Grant No: 1998K121480).

Appendix A. Supplementary data

CCDC 823467, 823468, 823465, and 823466 contain the supplementary crystallographic data for **3a**, **4a**, **5a**, and **2b**. These data can be obtained free of charge via http://www.ccdc.cam.ac.uk/conts/retrieving.html, or from the Cambridge Crystallographic Data Centre, 12 Union Road, Cambridge CB2 1EZ, UK; fax: +44 1223 336 033; or e-mail: deposit@ccdc.cam.ac.uk. Supplementary data associated with this article can be found, in the online version, at doi:10.1016/j.poly.2011.08.035.

References

[1] M. Işıklan, N. Asmafiliz, E.E. Özalp, E.E. İlter, Z. Kılıç, B. Çoşut, S. Yeşilot, A. Kılıç, A. Öztürk, T. Hökelek, L.Y. Koç, L.E. Akyüz, Inorg. Chem. 49 (2010) 7057.
[2] N. Asmafiliz, Z. Kılıç, A. Öztürk, T. Hökelek, L.Y. Koç, L. Açık, Ö. Kısa, A. Albay, Z. Üstündağ, A.O. Solak, Inorg. Chem. 48 (21) (2009) 10102.
[3] S. Bilge, Ş. Demiriz, A. Okumuş, Z. Kılıç, B. Tercan, T. Hökelek, O. Büyükgüngör, Inorg. Chem. 45 (2006) 8755.
[4] V. Chandrasekhar, P. Thilagar, B.M. Pandian, Coord. Chem. Rev. 251 (2007) 1045.
[5] A. Uslu, S.J. Coles, D.B. Davies, M. Esen, M.B. Hursthouse, A. Kılıç, İnorg. Chim. Acta 363 (2010) 3506.
[6] B. Çosut, F. Hacıvelioğlu, M. Durmuş, A. Kılıç, S. Yeşilot, Polyhedron 28 (2009) 2510.
[7] H.R. Allcock, Curr. Opin. Solid State Mater. Sci. 10 (2006) 231.
[8] M. Gleria, R.D. Jaeger, Phosphazenes a worldwide insight, Nova Science Publishers Inc., Hauppauge, New York, 2004.
[9] Z. Li, J. Qin, J. Polym. Sci., Part A: Polym. Chem. 42 (2004) 194.
[10] Z. Li, J. Qin, X. Xu, J. Polym. Sci., Part A: Polym. Chem. 42 (2004) 2877.
[11] G. Xu, Q. Lu, B. Yu, L. Wen, Solid State Ionics 177 (2006) 305.
[12] H.R. Allcock, R.M. Wood, J. Polym. Sci., Part B. Polym. Phys. 44 (2006) 2358.
[13] H.R. Allcock, M.E. Napierala, C.G. Cameron, S.J.M. O'Connor, Macromolecules 29 (1996) 1951.
[14] Z. Li, J. Qin, S. Li, C. Ye, J. Luo, Y. Cao, Macromolecules 35 (2002) 9232.
[15] Z. Li, C. Huang, J. Hua, J. Qin, Z. Yang, C. Ye, Macromolecules 37 (2004) 371.
[16] A. Singh, N.R. Krogman, S. Sethurman, L.S. Nair, J.L. Sturgeon, P.W. Brown, C.T. Laurencin, H.R. Allcock, Biomacromolecules 7 (2006) 914.
[17] Y.E. Greish, J.D. Bender, S. Lakshmi, P.W. Brown, H.R. Allcock, C.T. Laurencin, Biomaterials 26 (2005) 1.
[18] A. Okumuş, S. Bilge, Z. Kılıç, A. Öztürk, T. Hökelek, F. Yılmaz, Spectrochim. Acta Part A 76 (2010) 401.
[19] Z. Kılıç, A. Okumuş, Ş. Demiriz, S. Bilge, A. Öztürk, T. Hökelek, J. Inclusion Phenom. Macrocyclic Chem. 65 (2009) 269.
[20] S. Bilge, A. Natsagdorj, Ş. Demiriz, N. Çaylak, Z. Kılıç, T. Hökelek, Helv. Chim. Acta 87 (2004) 2088.
[21] S. Safran, T. Hökelek, S. Bilge, Ş. Demiriz, A. Natsagdorj, Z. Kılıç, Anal. Sci. 21 (2005) 77.
[22] B. Tercan, T. Hökelek, S. Bilge, A. Natsagdorj, Ş. Demiriz, Z. Kılıç, Acta Crystallogr. E60 (2004) 795.
[23] E.E. İlter, N. Asmafiliz, Z. Kılıç, L. Açık, M. Yavuz, E.B. Bali, A.O. Solak, F. Büyükkaya, H. Dal, T. Hökelek, Polyhedron 29 (2010) 2933.
[24] Bruker program 1D WIN-NMR (release 6.0) and 2D WIN-NMR (release 6.1).
[25] Z. Eckstein, A. Lukasiewicz, Przem. Chem. 39 (1960) 367.
[26] H.L. Zhu, X.Y. Qiu, S. Yang, J. Ma, Z. Kristallogr. New Cryst. Struct. 218 (2003) 523.
[27] Bruker, SADABS, Bruker AXS Inc., Madison, Wisconsin, USA, 2005.
[28] G.M. Sheldrick, SHELXS-97; SHELXL-97, University of Göttingen, Göttingen, Germany, 1997.
[29] V. Vicente, A. Fruchier, H.J. Cristau, Magn. Reson. Chem. 41 (2003) 183.
[30] S. Ramalingama, S. Periandyb, B. Elanchezhianc, S. Mohand, Spectrochim. Acta Part A 78 (2011) 429.
[31] E.E. İlter, N. Asmafiliz, Z. Kılıç, M. Işıklan, T. Hökelek, N. Çaylak, E. Şahin, Inorg. Chem. 46 (2007) 9931.
[32] G.A. Carriedo, F.G. Alonso, P.A. Gonzalez, J.R. Menendez, J. Raman Spectrosc. 29 (1998) 327.
[33] D. Cremer, J.A. Pople, J. Am. Chem. Soc. 97 (6) (1975) 1354.
[34] L.J. Farrugia, J. Appl. Crystallogr. 30 (1997) 565.
[35] F.H. Allen, O. Kennard, D.G. Watson, L. Brammer, G. Orpen, R.J. Taylor, J. Chem. Soc., Perkin Trans. 2 (12) (1987) 1.
[36] A.B. Chaplin, J.A. Harrison, P.J. Dyson, Inorg. Chem. 44 (2005) 8407.
[37] S.S. Krishnamurthy, Phosphorus, Sulfur Silicon Relat. Elem. 87 (1994) 101.
[38] G.J. Bullen, J. Chem. Soc. A. (1971) 1450.
[39] F. Gümüş, G. Eren, L. Açık, A. Çelebi, F. Öztürk, S. Yılmaz, R. Sağkan, S. Gür, A. Özkul, A. Elmalı, Y. Elerman, J. Med. Chem. 52 (2009) 1345.